A climate risk analysis of Earth's forests in the 21st century

Anderegg, William R. L.; Wu, Chao; Acil, Nezha; Carvalhais, Nuno; Pugh, Thomas A. M.; Sadler, Jon P.; Seidl, Rupert

DOI:
10.1126/science.abp9723

Citation for published version (Harvard):
Anderegg, WRL, Wu, C, Acil, N, Carvalhais, N, Pugh, TAM, Sadler, JP & Seidl, R 2022, 'A climate risk analysis of Earth's forests in the 21st century', *Science*, vol. 377, no. 6610, pp. 1099–1103. https://doi.org/10.1126/science.abp9723

A climate risk analysis of Earth's forests in the 21st century

William R. L. Anderegg[1,2]*, Chao Wu[2], Nezha Acil[3,4], Nuno Carvalhais[5,6], Thomas A. M. Pugh[3,4,7], Jon P. Sadler[3,4], Rupert Seidl[8,9]

[1]Wilkes Center for Climate Science and Policy, University of Utah, Salt Lake City, UT 84103 USA; [2]School of Biological Sciences, University of Utah, Salt Lake City, UT 84103 USA; [3]School of Geography Earth and Environmental Sciences, University of Birmingham, Birmingham, UK; [4]Birmingham Institute of Forest Research, University of Birmingham, Birmingham, U.K.; [5]Max Planck Institute for Biogeochemistry, Jena, Germany; [6]Departamento de Ciências e Engenharia do Ambiente, DCEA, Faculdade de Ciências e Tecnologia, FCT, Universidade Nova de Lisboa, 2829-516 Caparica, Portugal; [7]Department of Physical Geography and Ecosystem Science, Lund University, Lund, Sweden; [8]School of Life Sciences, Technical University of Munich, Freising, Germany; [9]Berchtesgaden National Park, Berchtesgaden, Germany.

Short title: Climate risks to forests

Key words: Carbon cycle feedback, drought, wildfire, disturbance, nature-based climate solutions

One Sentence Summary: A multi-method synthesis of climate risks to forests globally.

Abstract

Earth's forests harbor extensive biodiversity and are currently a major carbon sink. Forest conservation and restoration can help to mitigate climate change. Yet climate change could fundamentally imperil forests in many regions and undermine their ability to provide such mitigation. The extent of climate risks facing forests has not been synthesized globally, nor have different approaches to quantifying forest climate risks been systematically compared. Here we combine outputs from multiple mechanistic and empirical approaches to modeling carbon, biodiversity, and disturbance risks to conduct a synthetic climate risk analysis for Earth's forests in the 21st century. Despite large uncertainty in most regions, we find some forests consistently at higher risk, including southern boreal forests, western North America, and parts of the Amazon.

Main text

Earth's forests store carbon, support enormous terrestrial biodiversity, and provide trillions of dollars each year in ecosystem goods and services to society (*1*, *2*). Due to forests' potential carbon sequestration capacity and co-benefits, there is widespread and growing interest in leveraging forests for climate mitigation through nature-based climate solutions (*3*, *4*). Yet the future of forests globally is uncertain due to both land-use decisions and climate change (*5*–*7*). Forests face substantial climate risks that could trigger carbon-cycle feedbacks, accelerating climate change and fundamentally undermining their role in climate mitigation (*7*–*9*). Critical climate-sensitive risks to forest stability, biodiversity, and long-term carbon storage include disturbance triggered by extreme weather (e.g. fire, drought, hurricanes), biotic agents and invasive species, and large-scale demographic shifts (e.g. elevated mortality rates, species turnover, physiological limits to growth or regeneration) (*7*, *10*–*12*).

The large-scale and cross-biome patterns of climate risks to forests are not well-understood. With respect to ecosystems, the Intergovernmental Panel on Climate Change (IPCC) defines risk as the potential for adverse consequences for ecological systems and highlights that risk results from the dynamic interaction of climate-related hazards, exposure, susceptibility and (lack of) adaptive capacity of a system (*5*, *13*). Three major approaches have been used to examine key determinants of forest risk, each considering different processes, with distinct uncertainties and limitations. First, global mechanistic vegetation models, such as those included in Earth system models, simulate forest carbon fluxes and pools, climate impacts on those processes, some key climate-sensitive disturbances such as fire, and dynamic growth and recovery after disturbances (*14*, *15*). Second, 'climate envelope' approaches use empirical models based on relationships between observed climate patterns and forest attributes, such as biomass, species presence/abundance, or ecoregion/life-zone presence (*16–18*). Third, empirical assessments of climatic controls on stand-replacing disturbances, typically based on satellite data of forest loss or meta-analyses of field studies, are other common approaches (*11*, *19*). These major approaches roughly capture different ‘axes’ of forest climate risk to: (i) carbon stocks/storage (hereafter ‘C risk’), (ii) species composition changes (‘species risk’), and (iii) disturbance regime change (‘disturbance risk’). These approaches have different inherent strengths and weaknesses, but a synthesis of approaches at a global scale is lacking. A multi-method analysis to quantify risks spatially and estimate which regions may be particularly vulnerable in future climates is urgently needed to inform land management, conservation, and climate mitigation efforts.

Here, we compare results from these three types of approaches to provide a global assessment of climate risks facing Earth’s forests in the 21st century. We ask: i) what are the mean and uncertainty in projections of forest carbon storage and potential forest carbon losses in mechanistic vegetation models included in Earth system models (e.g. ‘C risk’), ii) what do empirical ‘climate envelope’ and ‘climate-sensitive disturbance’ approaches estimate for spatial and temporal climate risks to forests (e.g. ‘species risk’ and ‘disturbance risk’), and iii) what broader risk patterns emerge from the synthesis and comparisons of these three different axes of risks?

We first examined simulations of the live carbon in vegetation in forested areas (‘C risk’) from mechanistic vegetation models from the Coupled Model Intercomparison Project – Phase 6 (CMIP6: 23 models total, 13 with prognostic fire and 6 with dynamic vegetation, Table S1), removing the direct influences of human land use change, to contextualize overall forest carbon changes (*20*). Comparing 2081-2100 with 1995-2014, these models on average show carbon gains in currently forested areas in both high and low emissions scenarios (Fig. 1, Fig. S1). The multi-model mean was positive across most of the world, but with very high variation and uncertainty across models, particularly in the tropics and swaths of the boreal forests (Fig. 1A, 1B, Fig. S1). We examined relative agreement in spatial patterns of carbon gains and losses across models and found that spatial correlations across models for carbon changes were modest, with an average of r=0.30 across the 23 models considered here (Fig. S2).

We calculated two complementary metrics of potential climate C risk from these models as: 1) the number of models with carbon losses by 2081-2100 compared to 1995-2014 and 2) the percent change from tree functional types to other vegetation in a grid cell between those two periods for the subset of models (N=14) that reported data on vegetation change (*20*). The first metric uses the inherent variability in the model ensemble and assumes that the higher the number of models with C loss, the greater the risk, whereas the second metric directly calculates forest loss in models where it is represented. With the first metric, large areas of the Neotropics, the Mediterranean region and eastern Europe, as well as southwestern North America show notable risk (Fig. 1C). With the second metric, subtropical and southern boreal regions were more likely to lose tree functional types (Fig. 1D). We further found that these two metrics showed similar patterns of higher projected risk in southern boreal and drier regions in the Amazon and African tropics. Spatial patterns of carbon changes and climate risks were broadly similar between emissions scenarios (Fig. 1, Fig. S1) and between models with versus without prognostic fire simulated (Fig. S3).

We then examined forest 'species risk', estimated via empirical climate envelope models in three recently published papers. Using observed climate relationships at global scales, two papers estimated ecoregion/life-zone transitions (i.e. shifts from one ecoregion/life-zone to another) and the third modeled changes in forest species richness within a biome (*17*, *21*, *22*). Ecoregion transitions were projected to be most likely at current biome boundaries (sub-tropic – temperate, temperate – boreal, and tropical – subtropical biomes; Fig. 2A, 2B). We note that there could be similarly large transitions in terms of species composition within individual biomes, but that by their inherent ecoregion-focused structure the underlying analyses in Fig 2A-B would not capture community-level changes. Considering the third paper's analyses, risk of species loss estimates were highest in boreal regions and western North America and generally lower in tropical regions (Fig. 2C).

To quantify climate-sensitive 'disturbance risk', we used two complementary methods: 1) an empirical random-forest model linking observed climate to stand-replacing disturbance estimates based on satellite data from 2002-2014 with human land-use conversion removed (but harvest included, (*20*)), and 2) upscaled climate-dependent rates of disturbance in 103 protected areas from temperate and boreal biomes (*19*). For both methods, the models were built with observed relationships in the historical period. We estimated the change in stand-replacing disturbance rates using climate model output from the same 23 climate models we used for C risk for 2081-2100, with a moderate climate scenario (SSP2-4.5). The model of stand-replacing disturbances indicated that if current forests were exposed to projected future temperatures and precipitation, the largest increases of disturbance would be expected to occur in the tropics and southern boreal forests (Fig. 3A, 3B), whereas upscaled relationships from protected areas indicated high disturbance vulnerability broadly across boreal forests, although this dataset did not include tropical forests (Fig. 3B).

We emphasize that these three distinct axes of risk are capturing different aspects and dimensions of climate risks to forests, all of which are generally considered important responses of forests to climate change (*20*). The spatial and cross-biome relative risk patterns within each approach are likely what is most insightful and important in these comparisons, rather than the absolute values. Thus, we compared the spatial correlations in relative projected risk patterns with a correlation matrix and computed spatial covariation of risk percentiles across all metrics. Strikingly, none of the different metrics were significantly spatially correlated with each other ($p>0.05$), leading to high variability across risk metrics in many regions (Fig. S4), and the mechanistic vegetation model projections tended to be slightly negatively correlated with the other approaches (Fig. 4B). Despite this broad-scale disagreement, identification of regions that are at relatively higher or lower risk in a majority of approaches can still provide useful information for risk management. Aggregating risk metrics by the average percentile across all metrics with data in a given grid cell, southern boreal regions (e.g. central Canada) and drier regions of the tropics (e.g. southeast Amazonia) emerged as regions with higher than average risk across metrics, consistent with multiple observational studies (e.g. *23*, *24*). By contrast, eastern North America, western Amazonia, and southeast Asia exhibited lower than average risk (Fig. 4A, Fig. S5); a recent pan-tropical study also observed lower vulnerability in southeast Asian tropics (*25*). These regional patterns were generally robust in a sensitivity analysis that sequentially excluded individual risk maps (Fig. S6). Considering biome-wide patterns, tropical forests had slightly higher average median risk percentiles (51%ile and 62%ile for tropical moist broadleaf and tropical/subtropical dry broadleaf forests, respectively) than boreal (44%ile) or temperate (35%ile and 42%ile for broadleaf and coniferous, respectively) forests (Fig. S7).

All of the different approaches to estimating forest climate risk have limitations and different uncertainties that are worth bearing in mind. Mechanistic model projections (C risk axis) include the benefits of rising atmospheric CO_2 concentrations on forest productivity (i.e.

CO_2 fertilization), as well as coarse estimates of climate sensitivities of plant functional types and fire disturbance. However, these models are generally thought to be lacking a substantial range of key impacts of climate on tree mortality and other disturbances, making it likely that risk estimates from this approach are overly conservative and carbon gains may be overestimated (*26*). Furthermore, these models do not realistically capture current tropical forest carbon dynamics (*27*) and the potential for biome shifts remains very uncertain in these models (*14*, *28*), in part because they frequently neglect processes of tree regeneration (*29*).

The empirical species distribution and ecoregion biome transition models (species risk axis) are correlative in nature and do not directly include mechanistic processes of growth, mortality, CO_2-related effects, or disturbance. They are, nevertheless, widely used across the globe for conservation planning efforts (*16*, *30*), as they provide a powerful approach to estimate the species pool under given climatic conditions. Empirical disturbance models (disturbance risk axis) capture only one key component of forest carbon cycling and do not account for regrowth, species turnover, and other dynamics. Nonetheless, a broad body of literature has demonstrated that changes in disturbance regimes have strong leverage on forest carbon cycling in many ecosystems globally (*9*, *12*, *28*). Finally, all of these approaches treat direct human impacts of land-use change and management distinctly. Forest management, as a key disturbance and arbiter of forest risk, is included implicitly or explicitly in all methods here. Whilst we have made extensive efforts to screen out changes due to land conversion (*20*), land management remains an important uncertainty and caveat in these analyses. A previous global risk analysis for forest loss using a single, older mechanistic vegetation model (*31*) projected highest forest loss in the eastern Amazon, eastern North American boreal, and broad areas of the European and Asian boreal forests, which is partially consistent with the species turnover and biome transition estimates presented here (e.g. Fig 2A) and the multi-method aggregate map.

Ultimately, our analysis reveals a strikingly divergent set of projections when comparing across a wide range of methods and approaches to examine the vulnerability of Earth's forests to climate risks. If forests are tapped to play an important role in climate mitigation, an enormous scientific effort is needed to better shed light on when and where forests will be resilient to climate change in the 21st century. These results highlight an urgent need for more detailed treatment of climate-sensitive disturbances in mechanistic vegetation models, more extensive benchmarking of those models against disturbance and mortality datasets, and better identification of agents of change in observational datasets to underlie more nuanced empirical approaches. Continuing the long-term monitoring efforts that enable such work will be fundamental to improving such models. Our results also underscore key needs to focus on climate-driven biome transitions. Currently, enormous uncertainty remains about the spatial and temporal patterns of forest vulnerability to climate change. They further emphasize that the effectiveness of nature-based climate solutions currently under discussion (*3*, *4*) are faced with great uncertainties, given the profound climate impacts on forests expected in the 21st century.

References

1. G. B. Bonan, Forests and climate change: Forcings, feedbacks, and the climate benefits of forests. *Science*. **320**, 1444–1449 (2008).
2. FAO and UNEP, "The State of the World's Forests 2020. Forests, biodiversity and people" (Rome, 2020).
3. B. W. Griscom, J. Adams, P. W. Ellis, R. A. Houghton, G. Lomax, D. A. Miteva, W. H. Schlesinger, D. Shoch, J. V. Siikamäki, P. Smith, Natural climate solutions. *Proc. Natl. Acad. Sci.* **114**, 11645–11650 (2017).
4. S. Roe, C. Streck, M. Obersteiner, S. Frank, B. Griscom, L. Drouet, O. Fricko, M. Gusti, N. Harris, T. Hasegawa, Contribution of the land sector to a 1.5° C world. *Nat. Clim. Change*, 1–12 (2019).
5. IPCC, *Managing the Risks of Extreme Events and Disasters to Advance Climate Change Adaptation. A Special Report of Working Groups I and II of the Intergovernmental Panel on Climate Change* (Cambridge University Press, Cambridge, United Kingdom, and New York, NY, USA, 2012).
6. T. J. Brodribb, J. Powers, H. Cochard, B. Choat, Hanging by a thread? Forests and drought. *Science*. **368**, 261–266 (2020).
7. W. R. Anderegg, A. T. Trugman, G. Badgley, C. M. Anderson, A. Bartuska, P. Ciais, D. Cullenward, C. B. Field, J. Freeman, S. J. Goetz, Climate-driven risks to the climate mitigation potential of forests. *Science*. **368** (2020).
8. P. Friedlingstein, M. Meinshausen, V. K. Arora, C. D. Jones, A. Anav, S. K. Liddicoat, R. Knutti, Uncertainties in CMIP5 Climate Projections due to Carbon Cycle Feedbacks. *J. Clim.* **27** (2014).
9. W. A. Kurz, C. C. Dymond, G. Stinson, G. J. Rampley, E. T. Neilson, A. L. Carroll, T. Ebata, L. Safranyik, Mountain pine beetle and forest carbon feedback to climate change. *Nature*. **452**, 987–990 (2008).
10. C. D. Allen, A. K. Macalady, H. Chenchouni, D. Bachelet, N. McDowell, M. Vennetier, T. Kitzberger, A. Rigling, D. D. Breshears, E. H. Hogg, P. Gonzalez, R. Fensham, Z. Zhang, J. Castro, N. Demidova, J. H. Lim, G. Allard, S. W. Running, A. Semerci, N. Cobb, A global overview of drought and heat-induced tree mortality reveals emerging climate change risks for forests. *For. Ecol. Manag.* **259**, 660–684 (2010).
11. R. Seidl, D. Thom, M. Kautz, D. Martin-Benito, M. Peltoniemi, G. Vacchiano, J. Wild, D. Ascoli, M. Petr, J. Honkaniemi, Forest disturbances under climate change. *Nat. Clim. Change*. **7**, 395 (2017).
12. J. A. Wang, A. Baccini, M. Farina, J. T. Randerson, M. A. Friedl, Disturbance suppresses the aboveground carbon sink in North American boreal forests. *Nat. Clim. Change*. **11**, 435–441 (2021).
13. J. Lecina-Diaz, J. Martínez-Vilalta, A. Alvarez, M. Banqué, J. Birkmann, D. Feldmeyer, J. Vayreda, J. Retana, Characterizing forest vulnerability and risk to climate-change hazards. *Front. Ecol. Environ.* **19**, 126–133 (2021).
14. R. A. Fisher, C. D. Koven, W. R. Anderegg, B. O. Christoffersen, M. C. Dietze, C. E. Farrior, J. A. Holm, G. C. Hurtt, R. G. Knox, P. J. Lawrence, Vegetation demographics in Earth System Models: A review of progress and priorities. *Glob. Change Biol.* **24**, 35–54 (2018).
15. S. Hantson, D. I. Kelley, A. Arneth, S. P. Harrison, S. Archibald, D. Bachelet, M. Forrest,

T. Hickler, G. Lasslop, F. Li, Quantitative assessment of fire and vegetation properties in simulations with fire-enabled vegetation models from the Fire Model Intercomparison Project. *Geosci. Model Dev.* **13**, 3299–3318 (2020).

16. J. Elith*, C. H. Graham*, R. P. Anderson, M. Dudík, S. Ferrier, A. Guisan, R. J. Hijmans, F. Huettmann, J. R. Leathwick, A. Lehmann, J. Li, L. G. Lohmann, B. A. Loiselle, G. Manion, C. Moritz, M. Nakamura, Y. Nakazawa, J. McC. M. Overton, A. Townsend Peterson, S. J. Phillips, K. Richardson, R. Scachetti-Pereira, R. E. Schapire, J. Soberón, S. Williams, M. S. Wisz, N. E. Zimmermann, Novel methods improve prediction of species' distributions from occurrence data. *Ecography*. **29**, 129–151 (2006).
17. S. Z. Dobrowski, C. E. Littlefield, D. S. Lyons, C. Hollenberg, C. Carroll, S. A. Parks, J. T. Abatzoglou, K. Hegewisch, J. Gage, Protected-area targets could be undermined by climate change-driven shifts in ecoregions and biomes. *Commun. Earth Environ.* **2**, 1–11 (2021).
18. S. R. Coffield, K. S. Hemes, C. D. Koven, M. L. Goulden, J. T. Randerson, Climate-driven limits to future carbon storage in California's wildland ecosystems. *AGU Adv.*, 2(3), e2021AV000384 (2021).
19. R. Seidl, J. Honkaniemi, T. Aakala, A. Aleinikov, P. Angelstam, M. Bouchard, et al, Globally consistent climate sensitivity of natural disturbances across boreal and temperate forest ecosystems. *Ecography*. **43**, 967–978 (2020).
20. See Supplementary Methods and Materials.
21. A. S. Mori, L. E. Dee, A. Gonzalez, H. Ohashi, J. Cowles, A. J. Wright, M. Loreau, Y. Hautier, T. Newbold, P. B. Reich, Biodiversity–productivity relationships are key to nature-based climate solutions. *Nat. Clim. Change*. **11**, 543–550 (2021).
22. P. R. Elsen, E. C. Saxon, B. A. Simmons, M. Ward, B. A. Williams, H. S. Grantham, S. Kark, N. Levin, K.-V. Perez-Hammerle, A. E. Reside, Accelerated shifts in terrestrial life zones under rapid climate change. *Glob. Change Biol.* **28**, 918–935 (2022).
23. M. Michaelian, E.H. Hogg, R.J. Hall, E. Arsenault, Massive mortality of aspen following severe drought along the southern edge of the Canadian boreal forest. *Glob. Change Biol*, **17**, 2084-2094 (2011).
24. L.V. Gatti, L.S. Basso, J.B. Miller, M. Gloor, L. Gatti Domingues, H.L. Cassol, H. L., ... & R.A. Neves, Amazonia as a carbon source linked to deforestation and climate change. *Nature*, **595**, 388-393 (2021).
25. Saatchi S, Longo M, Xu L et al. Detecting vulnerability of humid tropical forests to multiple stressors. *One Earth*, **4**, 988-1003 (2021)
26. B. M. Sanderson, R. A. Fisher, A fiery wake-up call for climate science. *Nat. Clim. Change*. **10**, 175–177 (2020).
27. A. Koch, W. Hubau, S. L. Lewis, *Earths Future*, 9(5), e2020EF001874 (2021).
28. T. A. Pugh, A. Arneth, M. Kautz, B. Poulter, B. Smith, Important role of forest disturbances in the global biomass turnover and carbon sinks. *Nat. Geosci.* **12**, 730–735 (2019).
29. K. Albrich, W. Rammer, M. G. Turner, Z. Ratajczak, K. H. Braziunas, W. D. Hansen, R. Seidl, Simulating forest resilience: A review. *Glob. Ecol. Biogeogr.* **29**, 2082–2096 (2020).
30. L. L. Porfirio, R. M. Harris, E. C. Lefroy, S. Hugh, S. F. Gould, G. Lee, N. L. Bindoff, B. Mackey, Improving the use of species distribution models in conservation planning and

management under climate change. *PLoS One*. **9**, e113749 (2014).

31. M. Scholze, W. Knorr, N. W. Arnell, I. C. Prentice, A climate-change risk analysis for world ecosystems. *Proc. Natl. Acad. Sci.* **103**, 13116–13120 (2006).
32. M. A. Moritz, M.-A. Parisien, E. Batllori, M. A. Krawchuk, J. Van Dorn, D. J. Ganz, K. Hayhoe, Climate change and disruptions to global fire activity. *Ecosphere*. **3**, 1–22 (2012).
33. W. Knorr, A. Arneth, L. Jiang, Demographic controls of future global fire risk. *Nat. Clim. Change*. **6**, 781 (2016).
34. G. C. Hurtt, L. Chini, R. Sahajpal, S. Frolking, B. L. Bodirsky, K. Calvin, J. C. Doelman, J. Fisk, S. Fujimori, K. Klein Goldewijk, Harmonization of global land use change and management for the period 850–2100 (LUH2) for CMIP6. *Geosci. Model Dev.* **13**, 5425–5464 (2020).
35. M. Hansen, P. Potapov, R. Moore, M. Hancher, S. Turubanova, A. Tyukavina, D. Thau, S. Stehman, S. Goetz, T. Loveland, High-Resolution Global Maps of 21st-Century Forest Cover Change. *Science*. **342**, 850–853 (2013).
36. A. J. Meddens, J. A. Hicke, A. K. Macalady, P. C. Buotte, T. R. Cowles, C. D. Allen, Patterns and causes of observed piñon pine mortality in the southwestern United States. *New Phytol.* **206**, 91–97 (2015).
37. Y. Qin, J. T. Abatzoglou, S. Siebert, L. S. Huning, A. AghaKouchak, J. S. Mankin, C. Hong, D. Tong, S. J. Davis, N. D. Mueller, Agricultural risks from changing snowmelt. *Nat. Clim. Change*. **10**, 459–465 (2020).
38. L. R. Holdridge, Life zone ecology. *Life Zone Ecol.* (1967).
39. C. Parmesan, Ecological and evolutionary responses to recent climate change. *Annu Rev Ecol Evol Syst*. **37**, 637–669 (2006).
40. M. C. Urban, Accelerating extinction risk from climate change. *Science*. **348**, 571–573 (2015).
41. R. G. Pearson, Species' distribution modeling for conservation educators and practitioners. *Synth. Am. Mus. Nat. Hist.* **50**, 54–89 (2007).
42. L. L. Porfirio, R. M. Harris, E. C. Lefroy, S. Hugh, S. F. Gould, G. Lee, N. L. Bindoff, B. Mackey, Improving the use of species distribution models in conservation planning and management under climate change. *PLoS One*. **9**, e113749 (2014).
43. D. M. Olson, E. Dinerstein, E. D. Wikramanayake, N. D. Burgess, G. V. Powell, E. C. Underwood, J. A. D'amico, I. Itoua, H. E. Strand, J. C. Morrison, others, Terrestrial Ecoregions of the World: A New Map of Life on Earth: A new global map of terrestrial ecoregions provides an innovative tool for conserving biodiversity. *BioScience*. **51**, 933–938 (2001).
44. ESA, "Land Cover CCI Product User Guide Version 2" (Tech. Rep., 2017), (available at maps.elie.ucl.ac.be/CCI/viewer/download/ESACCI-LC-Ph2-PUGv2_2.0.pdf).
45. H. Hersbach, B. Bell, P. Berrisford, G. Biavati, A. Horányi, J. Muñoz Sabater, J. Nicolas, C. Peubey, R. Radu, I. Rozum, ERA5 hourly data on single levels from 1979 to present. *Copernic. Clim. Change Serv. C3S Clim. Data Store CDS*. **10** (2018).
46. S. A. Spawn, C. C. Sullivan, T. J. Lark, H. K. Gibbs, Harmonized global maps of above and belowground biomass carbon density in the year 2010. *Sci. Data*. **7**, 1–22 (2020).
47. F. Kimura, A. Kitoh, Downscaling by pseudo global warming method. *Final Rep. ICCAP*. **4346**, 435 (2007).

48. A. South, rworldmap: A New R package for Mapping Global Data. *R J.* **3** (2011) (available at http://www.academia.edu/download/30318942/rjournal_2011-1.pdf#page=35).
49. R. J. Hijmans, J. van Etten, raster: Geographic data analysis and modeling. *R Package Version*. **2**, 15 (2014).
50. P. Michna, M. Woods, RNetCDF–A Package for Reading and Writing NetCDF Datasets. *Peer-Rev. Open-Access Publ. R Found. Stat. Comput.*, 29 (2013).
51. A. Liaw, M. Wiener, L. Breiman, A. Cutler, Package "randomForest." *Retrieved Dec.* **12**, 2009 (2009).
52. T. Wei, V. Simko, M. Levy, Y. Xie, Y. Jin, J. Zemla, Package 'corrplot.' *Statistician*. **56**, e24 (2017).
53. R. Furrer, D. Nychka, S. Sain, M. D. Nychka, Package 'fields.' *R Found. Stat. Comput. Vienna Austria Httpwww Idg PlmirrorsCRANwebpackagesfieldsfields Pdf Last Accessed 22 Dec. 2012* (2009).
54. D. Adler, M. D. Adler, Package 'vioplot' (2021).
55. R. Bivand, T. Keitt, B. Rowlingson, E. Pebesma, M. Sumner, R. Hijmans, E. Rouault, M. R. Bivand, Package 'rgdal.' *Bind. Geospatial Data Abstr. Libr. Available Online Httpscran R-Proj. Orgwebpackagesrgdalindex Html Accessed 15 Oct. 2017* (2015).
56. G. Danabasoglu, NCAR CESM2 model output prepared for CMIP6 CMIP historical (2019), , doi:10.22033/ESGF/CMIP6.7627.
57. G. Danabasoglu, J.-F. Lamarque, J. Bacmeister, D. A. Bailey, A. K. DuVivier, J. Edwards, L. K. Emmons, J. Fasullo, R. Garcia, A. Gettelman, *J. Adv. Model. Earth Syst.*, in press.
58. G. Danabasoglu, NCAR CESM2-WACCM model output prepared for CMIP6 ScenarioMIP. *Earth Syst. Grid Fed. Httpsdoi Org1022033ESGFCMIP6*. **10026** (2019).
59. A. Cherchi, P. G. Fogli, T. Lovato, D. Peano, D. Iovino, S. Gualdi, S. Masina, E. Scoccimarro, S. Materia, A. Bellucci, Global mean climate and main patterns of variability in the CMCC-CM2 coupled model. *J. Adv. Model. Earth Syst.* **11**, 185–209 (2019).
60. T. Lovato, D. Peano, CMCC CMCC-CM2-SR5 Model Output Prepared for CMIP6 ScenarioMIP. *Earth Syst. Grid Fed.* (2020), doi:doi:10.22033/ESGF/CMIP6.1365.
61. R. Seferian, CNRM-CERFACS CNRM-ESM2-1 model output prepared for CMIP6 ScenarioMIP. *Earth Syst. Grid Fed. Httpsdoi Org1022033ESGFCMIP6*. **1395** (2019).
62. R. Séférian, P. Nabat, M. Michou, D. Saint-Martin, A. Voldoire, J. Colin, B. Decharme, C. Delire, S. Berthet, M. Chevallier, Evaluation of CNRM earth system model, CNRM-ESM2-1: Role of earth system processes in present-day and future climate. *J. Adv. Model. Earth Syst.* **11**, 4182–4227 (2019).
63. J.-C. Golaz, P. M. Caldwell, L. P. Van Roekel, M. R. Petersen, Q. Tang, J. D. Wolfe, G. Abeshu, V. Anantharaj, X. S. Asay-Davis, D. C. Bader, The DOE E3SM coupled model version 1: Overview and evaluation at standard resolution. *J. Adv. Model. Earth Syst.* **11**, 2089–2129 (2019).
64. D. C. Bader, et al, E3SM-Project E3SM1.1 Model Output Prepared for CMIP6 ScenarioMIP. *Earth Syst. Grid Fed.* (2020), doi:doi:10.22033/ESGF/CMIP6.15103.
65. EC-Earth Consortium, EC-Earth-Consortium EC-Earth3-CC Model Output Prepared for CMIP6 ScenarioMIP. *Earth Syst. Grid Fed.* (2021), doi:doi:10.22033/ESGF/CMIP6.15327.
66. R. Döscher, M. Acosta, A. Alessandri, P. Anthoni, A. Arneth, T. Arsouze, T. Bergmann, R. Bernadello, S. Bousetta, L.-P. Caron, The EC-earth3 Earth system model for the climate

model intercomparison project 6. *Geosci. Model Dev. Discuss.*, 1–90 (2021).

67. T. Mauritsen, J. Bader, T. Becker, J. Behrens, M. Bittner, R. Brokopf, V. Brovkin, M. Claussen, T. Crueger, M. Esch, Developments in the MPI-M Earth System Model version 1.2 (MPI-ESM1. 2) and its response to increasing CO2. *J. Adv. Model. Earth Syst.* **11**, 998–1038 (2019).
68. K. H. Wieners, M. Giorgetta, J. Jungclaus, C. Reick, M. Esch, M. Bittner, V. Gayler, H. Haak, P. de Vrese, T. Raddatz, MPI-M MPIESM1. 2-LR model output prepared for CMIP6 ScenarioMIP. *Earth Syst. Grid Fed. Httpsdoi Org1022033ESGFCMIP6*. **793** (2019).
69. Ø. Seland, M. Bentsen, D. Olivié, T. Toniazzo, A. Gjermundsen, L. S. Graff, J. B. Debernard, A. K. Gupta, Y.-C. He, A. Kirkevåg, Overview of the Norwegian Earth System Model (NorESM2) and key climate response of CMIP6 DECK, historical, and scenario simulations. *Geosci. Model Dev.* **13**, 6165–6200 (2020).
70. Ø. Seland, M. Bentsen, D. J. L. Olivìè, T. Toniazzo, A. Gjermundsen, L. S. Graff, J. B. Debernard, A. K. Gupta, Y. He, A. Kirkevåg, NCC NorESM2-LM model output prepared for CMIP6 ScenarioMIP ssp585 (2019).
71. M. Bentsen, D. J. L. Olivìè, y Seland, T. Toniazzo, A. Gjermundsen, L. S. Graff, M. Schulz, NCC NorESM2-MM model output prepared for CMIP6 ScenarioMIP. *Earth Syst. Grid Fed. URL Httpsdoi Org1022033ESGFCMIP6*. **608** (2019).
72. W.-L. Lee, Y.-C. Wang, C.-J. Shiu, I. -chun Tsai, C.-Y. Tu, Y.-Y. Lan, J.-P. Chen, H.-L. Pan, H.-H. Hsu, Taiwan Earth System Model Version 1: description and evaluation of mean state. *Geosci. Model Dev.* **13**, 3887–3904 (2020).
73. W.-L. Lee, H.-C. Liang, TaiESM1.0 Model Output Prepared for CMIP6 ScenarioMIP. *Earth Syst. Grid Fed.* (2020), doi:doi:10.22033/ESGF/CMIP6.9688.
74. T. Ziehn, M. A. Chamberlain, R. M. Law, A. Lenton, R. W. Bodman, M. Dix, L. Stevens, Y.-P. Wang, J. Srbinovsky, The Australian earth system model: ACCESS-ESM1. 5. *J. South. Hemisphere Earth Syst. Sci.* **70**, 193–214 (2020).
75. T. Ziehn, M. Chamberlain, A. Lenton, R. Law, R. Bodman, M. Dix, K. Druken, CSIRO ACCESS-ESM1. 5 model output prepared for CMIP6 ScenarioMIP ssp585. *Earth Syst. Grid Fed.* (2019).
76. T. Wu, Y. Lu, Y. Fang, X. Xin, L. Li, W. Li, W. Jie, J. Zhang, Y. Liu, L. Zhang, The Beijing Climate Center climate system model (BCC-CSM): the main progress from CMIP5 to CMIP6. *Geosci. Model Dev.* **12**, 1573–1600 (2019).
77. X. Xin, T. Wu, X. Shi, F. Zhang, J. Li, M. Chu, Q. Liu, J. Yan, Q. Ma, M. Wei, in *Version 20201101, Earth System Grid Federation* (2019).
78. N. C. Swart, J. N. Cole, V. V. Kharin, M. Lazare, J. F. Scinocca, N. P. Gillett, J. Anstey, V. Arora, J. R. Christian, S. Hanna, The Canadian Earth System Model version 5 (CanESM5. 0.3). *Geosci. Model Dev.* **12**, 4823–4873 (2019).
79. N. C. Swart, J. N. Cole, V. V. Kharin, M. Lazare, J. F. Scinocca, N. P. Gillett, J. Anstey, V. Arora, J. R. Christian, Y. Jiao, CCCma CanESM5 model output prepared for CMIP6 ScenarioMIP. *Earth Syst. Grid Fed.* (2019).
80. E. M. Volodin, E. V. Mortikov, S. V. Kostrykin, V. Y. Galin, V. N. Lykossov, A. S. Gritsun, N. A. Diansky, A. V. Gusev, N. G. Iakovlev, Simulation of the present-day climate with the climate model INMCM5. *Clim. Dyn.* **49**, 3715–3734 (2017).
81. E. Volodin, E. Mortikov, A. Gritsun, V. Lykossov, V. Galin, N. Diansky, A. Gusev, S. Kostrykin, N. Iakovlev, A. Shestakova, INM INM-CM4-8 model output prepared for

CMIP6 ScenarioMIP. *Earth Syst. Grid Fed. URL Httpsdoi Org1022033ESGFCMIP6*. **12321** (2019).
82. O. Boucher, J. Servonnat, A. L. Albright, O. Aumont, Y. Balkanski, V. Bastrikov, S. Bekki, R. Bonnet, S. Bony, L. Bopp, *J. Adv. Model. Earth Syst.*, in press.
83. O. Boucher, S. Denvil, G. Levavasseur, A. Cozic, A. Caubel, M. A. Foujols, Y. Meurdesoif, P. Cadule, M. Devilliers, E. Dupont, IPSL IPSL-CM6A-LR model output prepared for CMIP6 ScenarioMIP, Version 20200601 (2019).
84. Y. Kim, et al, KIOST KIOST-ESM Model Output Prepared for CMIP6 ScenarioMIP. *Earth Syst. Grid Fed.* (2019), doi:doi:10.22033/ESGF/CMIP6.11241.
85. T. Hajima, M. Watanabe, A. Yamamoto, H. Tatebe, M. A. Noguchi, M. Abe, R. Ohgaito, A. Ito, D. Yamazaki, H. Okajima, Development of the MIROC-ES2L Earth system model and the evaluation of biogeochemical processes and feedbacks. *Geosci. Model Dev.* **13**, 2197–2244 (2020).
86. K. Tachiiri, M. Abe, T. Hajima, O. Arakawa, T. Suzuki, Y. Komuro, K. Ogochi, M. Watanabe, A. Yamamoto, H. Tatebe, MIROC MIROC-ES2L model output prepared for CMIP6 ScenarioMIP. *Earth Syst. Grid Fed. Retrieved Httpcera-Www Dkrz DeWDCCmetaCMIP6CMIP6 ScenarioMIP MIROC MIROC-ES2L* (2019).
87. A. A. Sellar, J. Walton, C. G. Jones, R. Wood, N. L. Abraham, M. Andrejczuk, M. B. Andrews, T. Andrews, A. T. Archibald, L. de Mora, *J. Adv. Model. Earth Syst.*, in press.
88. P. Good, A. Sellar, Y. Tang, S. Rumbold, R. Ellis, D. Kelley, T. Kuhlbrodt, J. Walton, MOHC UKESM1. 0-LL model output prepared for CMIP6 ScenarioMIP. *Earth Syst. Grid Fed. Httpsdoi Org1022033ESGFCMIP6*. **1567** (2019).

Funding: WRLA acknowledges support from the David and Lucille Packard Foundation, US National Science Foundation grants 1802880, 2003017 and 2044937, and USDA National Institute of Food and Agriculture, Agricultural and Food Research Initiative Competitive Programme, Ecosystem Services and Agro-Ecosystem Management, grant no. 2018-67019-27850. CW acknowledges support from the David and Lucille Packard Foundation. RS, NA and TP acknowledge support from the European Research Council (ERC) under the European Union's Horizon 2020 research and innovation programme (RS: grant agreement No 101001905, FORWARD; NA and TP grant agreement No 758873, TreeMort). This study contributes to the strategic research areas BECC and MERGE.

Author contributions: WRLA designed the study with input from all co-authors. WRLA, CW, and NA analyzed the data. WRLA wrote an initial draft and CW, NA, NC, TAMP, JPS, and RS provided extensive comments and revisions.

Competing interests: The authors declare no competing interests.

Data and materials availability: Analysis code and processed data underlying the paper analyses can be found at https://figshare.com/s/b97c7071e2af904955e7. Google Earth Engine code for disturbance analysis can be found at: https://code.earthengine.google.com/?accept_repo=users/NXA807/ForestGlobalClimateRisks All CMIP6 data and datasets underlying the empirical model analysis are publicly available from the CMIP6 data portal or published article reference.

Supplementary Content

Materials and Methods

Figs. S1 to S10

Table S1

References (32-88)

Figures

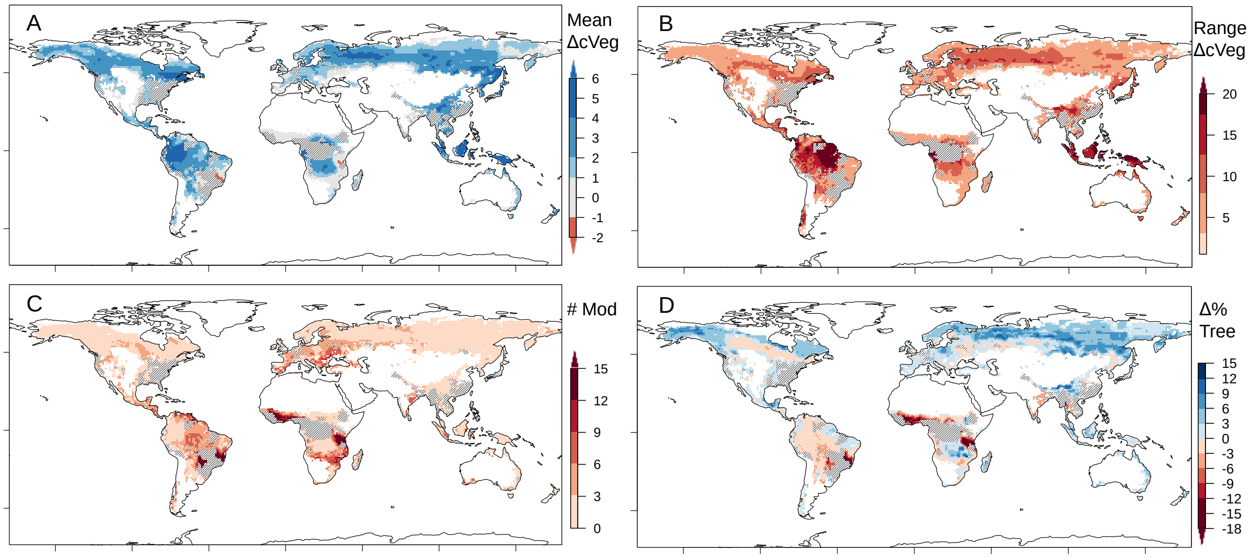

Figure 1: Future forest carbon and climate risk projections from mechanistic vegetation models. All panels analyze the change between 2081-2100 in Shared Socioeconomic Pathway 5-8.5 (SSP585) compared to 1995-2014 historical simulations and are masked by present forested areas. Multi-model mean (A) and range (B) of the change in live carbon mass in vegetation (kg*m^{-2}) across 23 models. (C) Number of models projecting vegetation carbon losses in a grid cell over the same time period. (D) Multi-model mean spatial patterns of the percent change in fraction of tree plant functional types in a grid cell. Gray hatched areas indicate grid cells removed from analysis due to land use-driven forest loss.

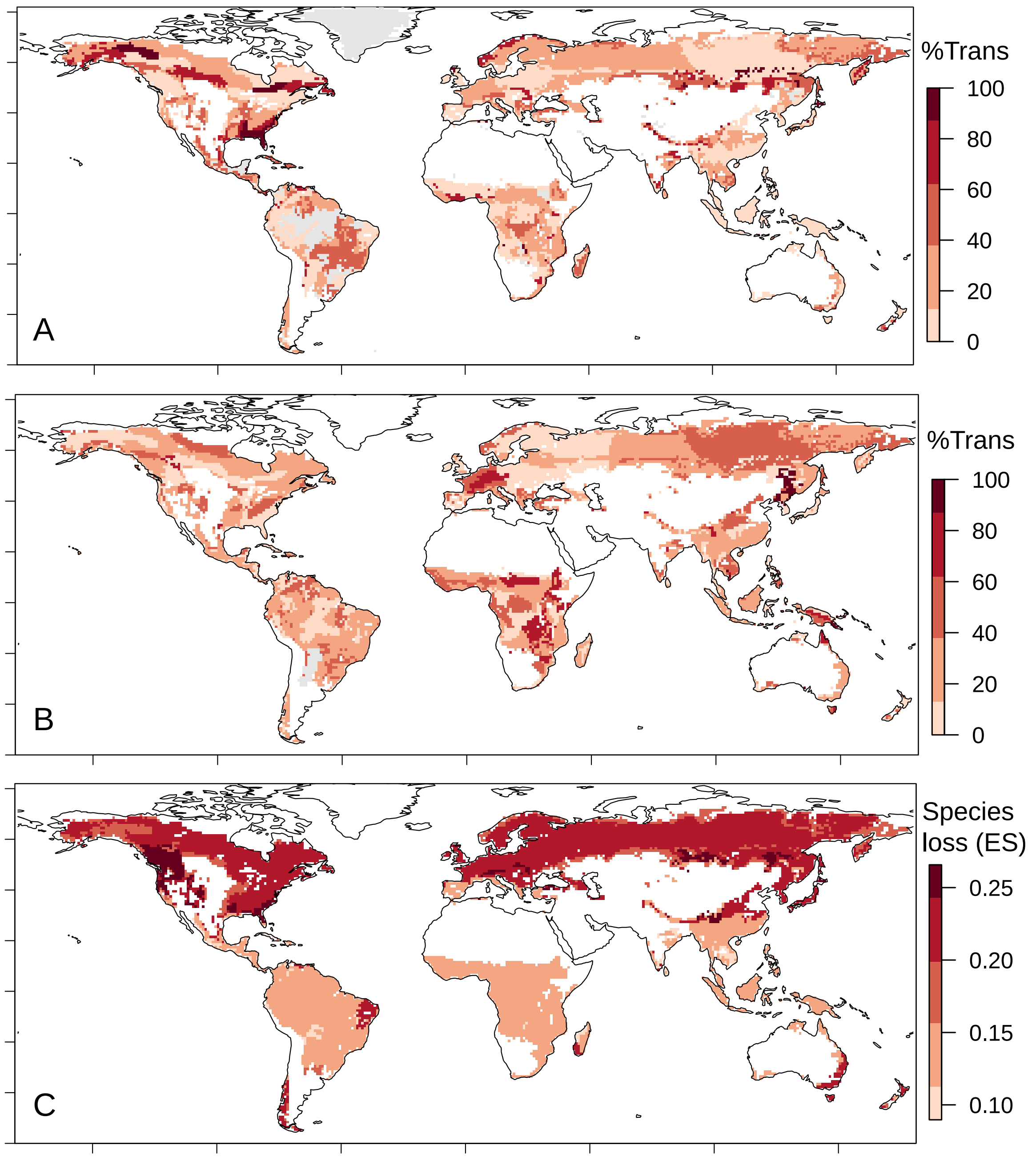

Figure 2: Global forest risk estimates from ‘climate envelope’ approaches. (A) Projected percent transition (%Trans) of ecoregions to another ecoregion with a warming of +2 C above pre-industrial from Dobrowski et al. 2021[17]. (B) Projected percent transition of climate ‘life-zones’ between 1979-2013 and 2061-2080 in a moderate (RCP 4.5) climate scenario from Elsen et al. 2021[21]. (C) Risk of loss in species richness (quantified as an ‘effect size’ (ES) of $-1 \times \log(\Delta SpeciesRichness_{highcc\text{-}mitigation}/\Delta SR_{baseline})$ where higher numbers indicate more risk of species loss) in the 2070s in a high climate change (RCP 8.5) scenario from Mori et al. 2021[20].

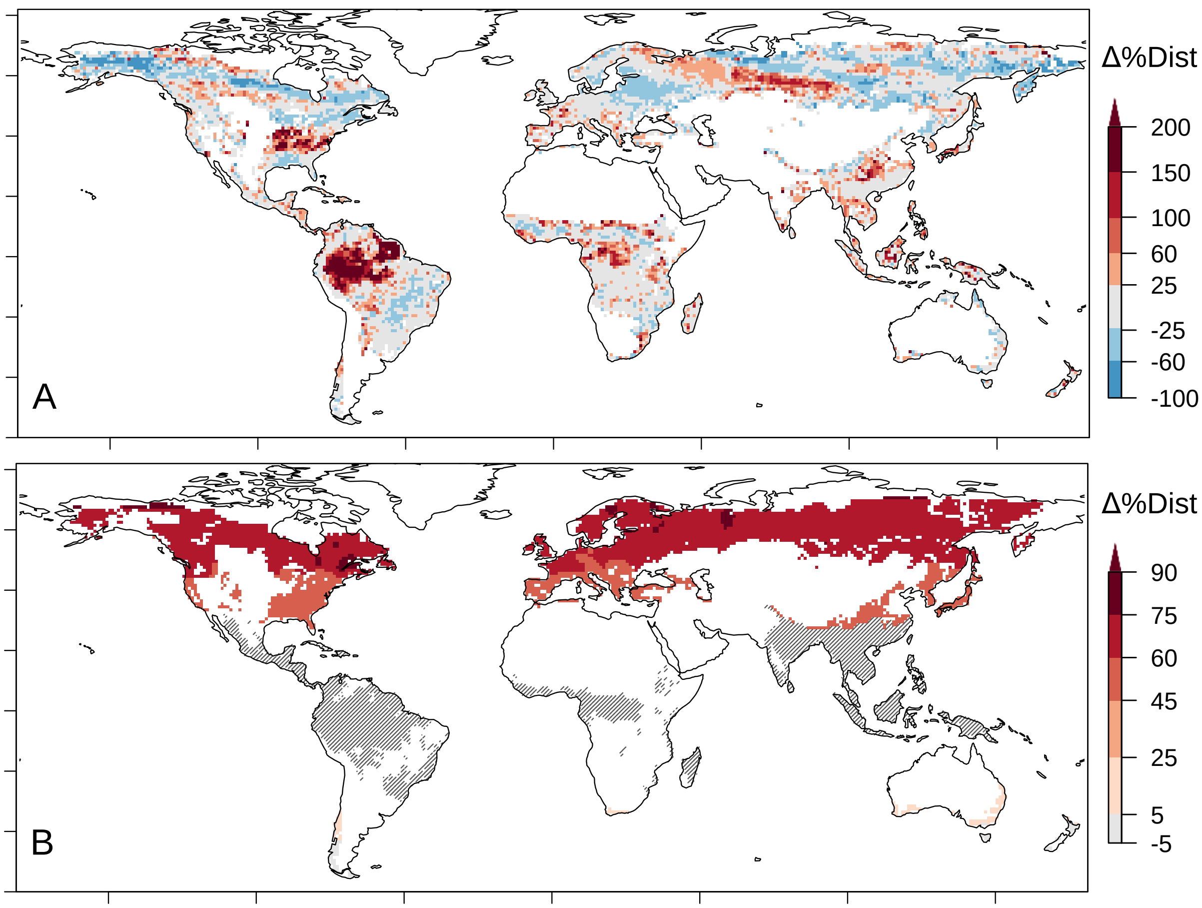

Figure 3: Projected change in climate-sensitive disturbance risks. (A) Average change in percent disturbed in a grid cell from random-forest model projections of Landsat-based stand-replacing disturbances for 2081-2100 in a moderate climate change scenario (Shared Socioeconomic Pathway 2-4.5 (SSP245)) compared to 1995-2014. (B) Average change in percent disturbed in a grid cell from protected area disturbance models for only temperate and boreal ecosystems in 2081-2100 in a moderate climate change scenario (SSP245) compared to 1995-2014. Gray hatching in grid cells indicates no data from this data source.

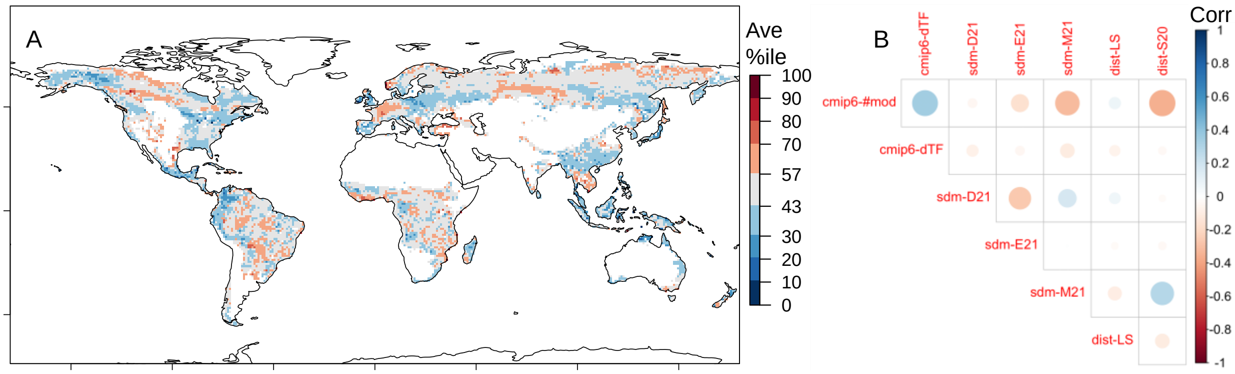

Figure 4: Comparisons and syntheses across different climate risk axes. (A) Average percentile of risk combined across all metrics where 0%ile is lowest climate risk and 100%ile is highest climate risk, averaged across all datasets that covered a given grid cell. (B) Correlation matrix between different climate risk axes and metrics where the size and color are proportionate to correlation strength and magnitude (all correlations n.s.). Risk axes and metrics: number of models showing carbon losses in forested regions in Coupled Model Intercomparison Project Phase 6 data (cmip6-#mod), change in tree fraction in the subset of CMIP6 models (cmip6-dTF), species distribution/climate niche models of ecoregion percent changes from Dobrowski et al. (2021)[17] (sdm-D21), species distribution/climate niche models of life-zone percent changes from Elsen et al. (2021)[20] (sdm-E21), species distribution models of loss of species richness from Mori et al. (2021)[21] (sdm-M21), random-forest based projections of Landsat-detected stand-replacing disturbances (dist-LS), and change in percent disturbed in a grid cell from protected area disturbance models from Seidl et al. (2020)[19] (dist-S20).